Two-dimensional non-separable quaternionic paraunitary filter banks

Nick A. Petrovsky Eugene V. Rybenkov Alexander A. Petrovsky

nick.petrovsky@bsuir.by

September 19, 2018

Belarusian State University of Informatics and Radioelectronics,
Department of Computer Engineering
Minsk, BELARUS

22st Conference SPA 2018
Signal Processing: Algorithms, Architectures, Arrangements, and Applications
September 19th - 21st, 2018, Poznań, POLAND

Motivation

1. The rapid development of the Internet, wireless communication, and portable computing, the demands for and the interests in digital multimedia (digitized speech, audio, image, video, computer graphics, and their combination) are growing exponentially.
2. A high-performance filter bank (FB) is typically at the heart of every state-of-the-art digital multimedia system.
3. The linear phase (LP) and paraunitary properties of filter banks are particularly significant for the subband coding of images.
4. One-dimensional linear phase paraunitary filter banks (LP PUFB) can be applied to the construction of multidimensional separable systems.
5. Multidimensional signals are generally non-separable, and 1-D approach does not exploit their characteristics effectively.

Filter banks as kernel for decorrelation transforms

Uniform maximally decimated M-channel filter bank:

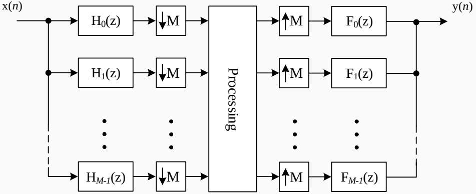

$$[H_0(z) \quad H_1(z) \quad \dots \quad H_{M-1}(z)] = \mathbf{E}(z^M)\mathbf{e}(z)^T,$$
$$[F_0(z) \quad F_1(z) \quad \dots \quad F_{M-1}(z)] = \mathbf{e}(z)\mathbf{R}(z^M),$$

The polyphase representation based on the $\mathbf{E}(z)$ и $\mathbf{R}(z)$:

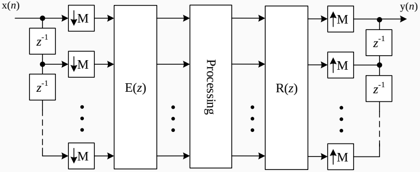

Biorthogonal filter bank (BOFB):

$$\mathbf{R}(z)\mathbf{E}(z) = bz^{-l}\mathbf{I}, b \neq 0, l \geq 0$$

Paraunitary filter bank (PUFB):

$$\mathbf{E}^T(z^{-1})\mathbf{E}(z) = \mathbf{I}, \mathbf{R}(z) = \mathbf{E}^T(z^{-1})$$

Taking into account the advantages of the Q-PUFB the aim of this paper is to show a novel technique of factorization for 2-D non-separable quaternionic paraunitary filter banks (2D-NSQ-PUFB) and evaluate their performance.

Design examples show that non-separable transform have better frequency characteristics and energy compaction.

Conventional 2-D transform

Separable ("Conventional") 2-D transform based on the 1-D transform

General case for 1-D transform $\mathbf{y}_{n,n} = \mathbf{\Theta}_{n,n} \cdot \mathbf{x}_{n,n}$ where $\mathbf{x}_{n,n}$ is 2-D input signal, $\mathbf{\Theta}_{n,n}$ — conversion matrix, whose size is $n \times n$, $\mathbf{y}_{n,n}$ is transformation result $n \times n$.

The two-dimensional transform based on the orthogonal transform $\mathbf{\Theta}_{n,n}$ applied to 2D input signal $\mathbf{x}_{n,n}$ separately by column and row

$$\mathbf{y}_{n,n} = \mathbf{\Theta}_{n,n} \cdot \mathbf{x}_{n,n} \cdot \mathbf{\Theta}_{n,n}^T$$

Intermediate result $\mathbf{x}_{n,n}\mathbf{\Theta}_{n,n}^T$, require additional memory of size $n \times n$.

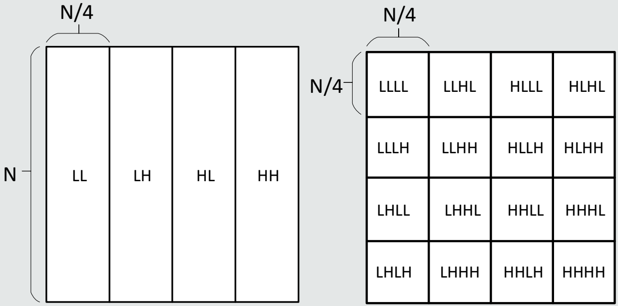

Memory-efficient high-throughput 2-D filter banks

Definition 1.

$$\left[\mathbf{x}_{1,1}\ldots\mathbf{x}_{1,n}\ldots\mathbf{x}_{n,1}\ldots\mathbf{x}_{n,n}\right]^T \underleftarrow{\mathrm{tv}} \begin{bmatrix}\mathbf{x}_{1,1} & \cdots & \mathbf{x}_{1,n}\\ \vdots & \ddots & \vdots\\ \mathbf{x}_{n,1} & \cdots & \mathbf{x}_{n,n}\end{bmatrix}$$

where $\mathrm{tv}\left(\mathbf{x}_{n,n}\right)$ denotes the forward transformation: $\mathbf{x}_{n\cdot n,1} = \mathrm{tv}\left(\mathbf{x}_{n,n}\right)$.

Definition 2.

The inverse transform $\mathbf{x}_{n,n} = \overline{\mathrm{tv}}\left(\mathbf{x}_{n\cdot n,1}\right)$ for the vector $\mathbf{x}_{n\cdot n,1}$ is defined as:

$$\begin{bmatrix}\mathbf{x}_{1,1} & \cdots & \mathbf{x}_{1,n}\\ \vdots & \ddots & \vdots\\ \mathbf{x}_{n,1} & \cdots & \mathbf{x}_{n,n}\end{bmatrix} \underleftarrow{\overline{\mathrm{tv}}} \left[\mathbf{x}_{1,1}\ldots\mathbf{x}_{1,n}\ldots\mathbf{x}_{n,1}\ldots\mathbf{x}_{n,n}\right]^T.$$

Definition 3.

The forward transform of the transposed matrix $\mathbf{x}_{n,n}^T$ is $\mathbf{z}_{n\cdot n,1} = \mathrm{tv}\left(\mathbf{x}_{n,n}^T\right)$:

$$\left[\mathbf{x}_{1,1}\ldots\mathbf{x}_{n,1}\ldots\mathbf{x}_{1,n}\ldots\mathbf{x}_{n,n}\right]^T \underleftarrow{\mathrm{tv}} \begin{bmatrix}\mathbf{x}_{1,1} & \cdots & \mathbf{x}_{n,1}\\ \vdots & \ddots & \vdots\\ \mathbf{x}_{1,n} & \cdots & \mathbf{x}_{n,n}\end{bmatrix}$$

Memory-efficient high-throughput 2-D filter banks

Based on the def. 1, the vectors $\mathbf{z}_{n\cdot n,1}$, $\mathbf{x}_{n\cdot n,1}$ and matrix $\mathbf{x}_{n,n}$ are related as follows:

$$\mathbf{z}_{n\cdot n,1} = \mathbf{P}\cdot\mathbf{x}_{n\cdot n,1} = \mathbf{P}\cdot\operatorname{tv}\left(\mathbf{x}_{n,n}\right), \quad \operatorname{tv}\left(\mathbf{x}_{n,n}^{T}\right) = \mathbf{P}\cdot\operatorname{tv}\left(\mathbf{x}_{n,n}\right),$$

where $\mathbf{P}$ is the permutation matrix of size $(n^2\times n^2)$.

Theorem 4.

The factorization of memory-efficient high-throughput 2D separable transform is

$$\mathbf{y}_{n\cdot n,1} = \boldsymbol{\Theta}_{\text{diag}}\cdot\mathbf{P}\cdot\boldsymbol{\Theta}_{\text{diag}}\cdot\mathbf{P}\cdot\mathbf{x}_{n\cdot n,1} = \ddot{\boldsymbol{\Theta}}_{n^2,n^2}\cdot\mathbf{x}_{n\cdot n,1},$$

$$\ddot{\boldsymbol{\Theta}}_{n^2,n^2} = \boldsymbol{\Theta}_{\text{diag}}\cdot\mathbf{P}\cdot\boldsymbol{\Theta}_{\text{diag}}\cdot\mathbf{P}$$

Proof.

Two-dimensional transformation can be rewritten as

$$\mathbf{y}_{n,n} = \boldsymbol{\Theta}_{n,n}\cdot\mathbf{x}_{n,n}\cdot\boldsymbol{\Theta}_{n,n}^{T} = \boldsymbol{\Theta}_{n,n}\cdot\left(\boldsymbol{\Theta}_{n,n}\cdot\mathbf{x}_{n,n}^{T}\right)^{T}.$$

By applying permutation matrix $\mathbf{P}$

$$\mathbf{y}_{n\cdot n,1} = \begin{bmatrix}\boldsymbol{\Theta}_{n,n} & \cdots & \mathbf{0}\\ \vdots & \ddots & \vdots\\ \mathbf{0} & \cdots & \boldsymbol{\Theta}_{n,n}\end{bmatrix}\cdot\mathbf{P}\cdot\begin{bmatrix}\boldsymbol{\Theta}_{n,n} & \cdots & \mathbf{0}\\ \vdots & \ddots & \vdots\\ \mathbf{0} & \cdots & \boldsymbol{\Theta}_{n,n}\end{bmatrix}\cdot\mathbf{P}\cdot\mathbf{x}_{n\cdot n,1}.$$

$\square$

Steps of image processing in parallel-pipeline processor 2D separable 4-band filter bank

2D separable M-channel FB ($M = 4$) with polyphase matrix $\mathbf{E}$:

$$\mathbf{y}_{M\cdot M,1} = \mathrm{diag}\left(\mathbf{E},\mathbf{E},\mathbf{E},\mathbf{E}\right)\cdot\mathbf{P}\cdot\mathrm{diag}\left(\mathbf{E},\mathbf{E},\mathbf{E},\mathbf{E}\right)\cdot\mathbf{P}\cdot\mathbf{x}_{M\cdot M,1}.$$

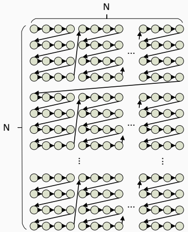

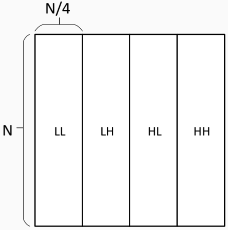

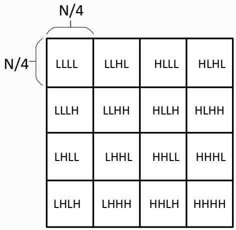

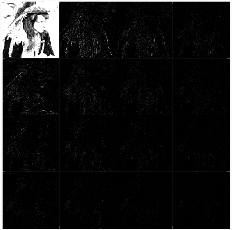

Quaternion algebra and orthogonal matrices

The quaternion algebra $\mathbb{H}$ is an associative non-commutative four-dimensional algebra

$$\mathbb{H} = \{\mathbf{q} = q_1 + q_2 i + q_3 j + q_4 k | q_1, q_2, q_3, q_4 \in \mathbb{R}\},$$

where the orthogonal imaginary numbers obey the following multiplicative rules:

$$i^2 = j^2 = k^2 = ijk = -1,\ ij = -ji = k, jk = -kj = i,\ ki = -ik = j.$$

There are two different multiplication matrices $\mathbf{M}^+ (q)$ and $\mathbf{M}^- (q)$:

$$qx \Leftrightarrow \mathbf{M}^+ (q)\, \mathbf{x}, \quad xq \Leftrightarrow \mathbf{M}^- (q)\, \mathbf{x}$$

$$\mathbf{M}^+ (P) = \begin{bmatrix} p_1 & -p_2 & -p_3 & -p_4 \\ p_2 & p_1 & -p_4 & p_3 \\ p_3 & p_4 & p_1 & -p_2 \\ p_4 & -p_3 & p_2 & p_1 \end{bmatrix}, \mathbf{M}^- (Q) = \begin{bmatrix} q_1 & -q_2 & -q_3 & -q_4 \\ q_2 & q_1 & q_4 & -q_3 \\ q_3 & -q_4 & q_1 & q_2 \\ q_4 & q_3 & -q_2 & q_1 \end{bmatrix}$$

Every matrix belonging to $SO(4)$, can be represented as a product of left and right unit quaternions P and Q ($|P| = 1$ and $|Q| = 1$)

$$\underset{\mathbf{R} \in SO(4)}{\forall} \ \underset{P,Q \in \text{unit quat.}}{\exists} \quad \mathbf{R} = \mathbf{M}^+ (P) \cdot \mathbf{M}^- (Q) = \mathbf{M}^- (Q) \cdot \mathbf{M}^+ (P)$$

Quaternionic critically sampled linear phase with pairwise-mirror-image (PMI) symmetric frequency responses PMI LP PUFB

Structurally lossless lattice for Q-PUFB [1,2]

$$\mathbf{E}(z) = \mathbf{G}_{N-1}\mathbf{G}_{N-2}\ldots\mathbf{G}_1\mathbf{E}_0;$$

$$\mathbf{E}_0 = \frac{1}{\sqrt{2}}\mathbf{\Phi}_0\mathbf{W}\,\mathrm{diag}\left(\mathbf{I}_{M/2},\mathbf{J}_{M/2}\right),\ \mathbf{G}_i = \frac{1}{2}\mathbf{\Phi}_i\mathbf{W}\mathbf{\Lambda}(z)\mathbf{W},\quad i=\overline{1,N-1},$$

$$\mathbf{W} = \begin{bmatrix}\mathbf{I}_{M/2} & \mathbf{I}_{M/2}\\ \mathbf{I}_{M/2} & -\mathbf{I}_{M/2}\end{bmatrix};\ \mathbf{\Lambda}(z) = \mathrm{diag}\left(\mathbf{I}_{M/2}, z^{-1}\mathbf{I}_{M/2}\right),$$

$$\mathbf{\Phi}_i = \mathrm{diag}\left(\mathbf{\Gamma}_{M/2},\mathbf{I}_{M/2}\right)\cdot\begin{bmatrix}\mathbf{M}^-(Q_i) & \\ & \mathbf{M}^-(Q_i)\end{bmatrix}\cdot\begin{bmatrix}\mathbf{M}^+(P_i) & \\ & \mathbf{M}^+(P_i)\end{bmatrix}\cdot\mathrm{diag}\left(\mathbf{\Gamma}_{M/2},\mathbf{I}_{M/2}\right)$$

$$\mathbf{\Phi}_{N-1} = \mathrm{diag}\left(\mathbf{J}_{M/2},\mathbf{I}_{M/2}\right)\cdot\begin{bmatrix}\mathbf{M}^-(Q_i) & \\ & \mathbf{M}^-(Q_i)\end{bmatrix}\cdot\begin{bmatrix}\mathbf{M}^+(P_i) & \\ & \mathbf{M}^+(P_i)\end{bmatrix}\cdot\mathrm{diag}\left(\mathbf{\Gamma}_{M/2},\mathbf{I}_{M/2}\right)$$

where N is order of the factorization; $\mathbf{I}_{M/2}$ and $\mathbf{J}_{M/2}$ denote the $M/2\times M/2$ identity and reversal matrices, respectively; $\mathbf{\Gamma}_{M/2}$ is diagonal matrix the elements of which are defined as $\gamma_{mm} = (-1)^{m-1}$, $m=\overline{1,M-1}$.

[1] M. Parfieniuk and A. Petrovsky, "Quaternionic lattice structures for four-channel paraunitary filter banks," *EURASIP J. Adv. Signal Process., Special Issue on Multirate Systems and Applications*., vol. 2007, Article ID 37481.

[2] M. Parfieniuk and A. Petrovsky, "Inherently lossless structures for eight and six-channel linear-phase paraunitary filter banks based on quaternion multipliers," *Signal Process.*, vol. 90, pp. 1755–1767, 2010.

Two-dimensional non-separable PMI LP Q-PUFB

When a factorization of PMI LP Q-PUFB matrix $\mathbf{E}$ is applied to a 2D input signal

$$\mathbf{y}_{n,n} = \mathbf{E} \cdot \mathbf{x}_{n,n} \cdot \mathbf{E}^T = \mathbf{G}_{N-1} \dots \mathbf{G}_1 \mathbf{E}_0 \cdot \mathbf{x}_{n,n} \cdot \mathbf{E}_0^T \mathbf{G}_1^T \dots \mathbf{G}_{N-1}^T,$$

This means that the 2D implementation of $\mathbf{G}_k$ is performed after that of $\mathbf{G}_{k-1}$ $(1 \leq k \leq N-1)$, i.e., the matrices $\mathbf{W}$, $\mathbf{\Lambda}(z)$, $\mathbf{M}^+\ (P)$ can be operated separately.

Sequence of matrix replacement for PMI LP Q-PUFB

$$\mathbf{y}_{n,n} = \dots \cdot \underline{\mathrm{diag}\left(\mathbf{I}_{M/2}, \mathbf{J}_{M/2}\right) \cdot \underline{\mathbf{W} \cdot \underline{\mathbf{\Phi}_0 \underline{\frac{1}{\sqrt{2}} \mathbf{x}_{n,n} \frac{1}{\sqrt{2}}} \mathbf{\Phi}_0^T} \cdot \mathbf{W}^T} \cdot \mathrm{diag}\left(\mathbf{I}_{M/2}, \mathbf{J}_{M/2}\right)^T} \cdot \dots$$

Rewritten 2D non-separable PMI LP Q-PUFB is

$$\mathbf{y}_{n \cdot n,1} = \ddot{\mathbf{E}} \cdot \mathbf{x}_{n \cdot n,1} = \ddot{\mathbf{G}}_{N-1}(z) \ddot{\mathbf{G}}_{N-2}(z) \cdot \dots \cdot \ddot{\mathbf{G}}_1(z) \cdot \ddot{\mathbf{E}}_0 \cdot \mathbf{x}_{n \cdot n,1},$$

where $\ddot{}$ denotes the 2D-transformation matrix.

Two-dimensional non-separable PMI LP Q-PUFB

Representation of 2D matrices ($\mathbf{W}$)

$$\ddot{\mathbf{W}} = \begin{bmatrix} \mathbf{W}_M & \cdots & \mathbf{0} \\ \vdots & \ddots & \vdots \\ \mathbf{0} & \cdots & \mathbf{W}_M \end{bmatrix} \cdot \mathbf{P} \cdot \begin{bmatrix} \mathbf{W}_M & \cdots & \mathbf{0} \\ \vdots & \ddots & \vdots \\ \mathbf{0} & \cdots & \mathbf{W}_M \end{bmatrix} \cdot \mathbf{P};$$

$$\ddot{\mathbf{W}} = \begin{bmatrix} \mathbf{W}_M & \cdots & \mathbf{0} \\ \vdots & \ddots & \vdots \\ \mathbf{0} & \cdots & \mathbf{W}_M \end{bmatrix} \cdot \mathbf{W}_{4\cdot M}, \mathbf{W}_{4\cdot M} = \begin{bmatrix} \mathbf{I}_{2\cdot M} & \mathbf{I}_{2\cdot M} \\ \mathbf{I}_{2\cdot M} & -\mathbf{I}_{2\cdot M} \end{bmatrix} = \mathbf{P} \cdot \begin{bmatrix} \mathbf{W}_M & \cdots & \mathbf{0} \\ \vdots & \ddots & \vdots \\ \mathbf{0} & \cdots & \mathbf{W}_M \end{bmatrix} \cdot \mathbf{P}$$

And for $\mathbf{\Lambda}$:

$$\ddot{\mathbf{\Lambda}}(z) = \begin{bmatrix} \mathbf{\Lambda}_M(z) & \cdots & \mathbf{0} \\ \vdots & \ddots & \vdots \\ \mathbf{0} & \cdots & \mathbf{\Lambda}_M(z) \end{bmatrix} \cdot \mathbf{P} \cdot \begin{bmatrix} \mathbf{\Lambda}_M(z) & \cdots & \mathbf{0} \\ \vdots & \ddots & \vdots \\ \mathbf{0} & \cdots & \mathbf{\Lambda}_M(z) \end{bmatrix} \cdot \mathbf{P};$$

$$\ddot{\mathbf{\Lambda}} = \begin{bmatrix} \mathbf{\Lambda}_M & \cdots & \mathbf{0} \\ \vdots & \ddots & \vdots \\ \mathbf{0} & \cdots & \mathbf{\Lambda}_M \end{bmatrix} \cdot \mathbf{\Lambda}_{4\cdot M}, \quad \mathbf{\Lambda}_{4\cdot M} = \mathbf{P} \cdot \begin{bmatrix} \mathbf{\Lambda}_M & \cdots & \mathbf{0} \\ \vdots & \ddots & \vdots \\ \mathbf{0} & \cdots & \mathbf{\Lambda}_M \end{bmatrix} \cdot \mathbf{P};$$

Two-dimensional non-separable PMI LP Q-PUFB

For 4-channel LP PMI Q-PUFB

$$\ddot{\boldsymbol{\Phi}}_i = \begin{bmatrix} \mathbf{M}^+(P_i) & 0 & 0 & 0 \\ 0 & \mathbf{M}^+(P_i) & 0 & 0 \\ 0 & 0 & \mathbf{M}^+(P_i) & 0 \\ 0 & 0 & 0 & \mathbf{M}^+(P_i) \end{bmatrix} \cdot \mathbf{P} \times$$

$$\times \begin{bmatrix} \mathbf{M}^+(P_i) & 0 & 0 & 0 \\ 0 & \mathbf{M}^+(P_i) & 0 & 0 \\ 0 & 0 & \mathbf{M}^+(P_i) & 0 \\ 0 & 0 & 0 & \mathbf{M}^+(P_i) \end{bmatrix} \cdot \mathbf{P}$$

$$\begin{aligned} \ddot{\boldsymbol{\Phi}}_{N-1} &= \ddot{\boldsymbol{\Phi}}_i \cdot \ddot{\mathbf{S}}_i, \\ \ddot{\mathbf{S}} &= \operatorname{diag}(\mathbf{S}_1, \mathbf{S}_1, \mathbf{S}_1, \mathbf{S}_1) \cdot \mathbf{P} \operatorname{diag}(\mathbf{S}_1, \mathbf{S}_1, \mathbf{S}_1, \mathbf{S}_1) \cdot \mathbf{P}, \\ \mathbf{S}_1 &= \operatorname{diag}\left(\mathbf{J}_{M/2} \cdot \boldsymbol{\Gamma}_{M/2}, \mathbf{I}_{M/2}\right) \end{aligned}$$

Similarly, the 2D non-separable factorization for the 8-channel PMI LP Q-PUFB can be found.

The structure of the critically sampled 2-D non-separable PMI LP Q-PUFB for $N = 1$

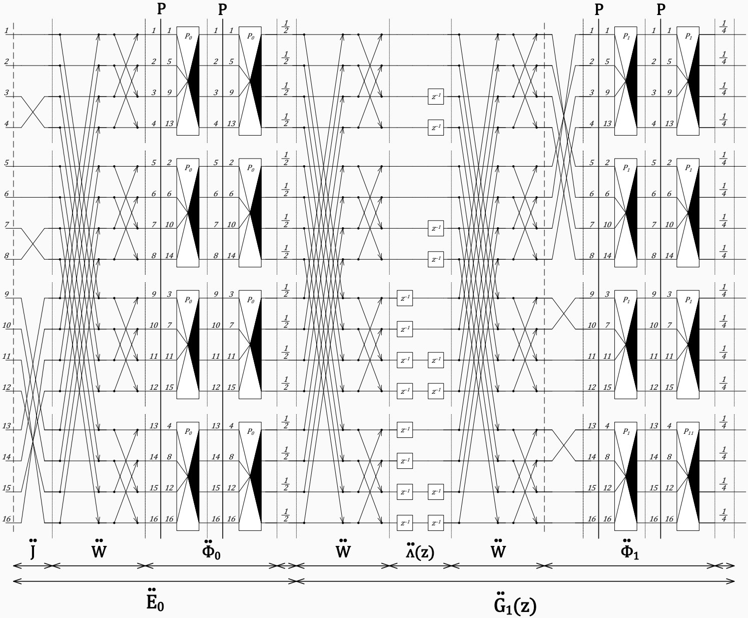

Filter bank synthesis: general algorithm steps

1. Set the initial values (initial point x, penalty coefficients increment, order of factorization N)
2. Find unconstrained maximum of function $f(x^{\star}) = \max_{x \in X} CG(\sigma_{xk}^2)$

$$CG = 10 \log_{10} \left(\frac{\frac{1}{M} \sum_{k=0}^{M-1} \sigma_{xk}^2}{\left(\prod_{k=0}^{M-1} \sigma_{xk}^2 \right)^{\frac{1}{M}}} \right),$$

σ_{xk}^2 are the subband variances,

using gradient descent method.

3. End

The coding gain CG_{MD} of 2-D non-separable PMI LP Q-PUFB with rectangular decimation for the isotropic autocorrelation function model with the correlation factor $\rho = 0.95$

Decimation factor	Structure 2-D NSQ-PUFB	CG_{1D} [dB]	CG_{MD} [dB]	
			1-D	2-D
$\begin{bmatrix} 4 & 0 \\ 0 & 4 \end{bmatrix}$	16in-16out	8.19	13.36	14.58
$\begin{bmatrix} 8 & 0 \\ 0 & 8 \end{bmatrix}$	64in-64out	9.38	15.54	17.12

Basis images of 16 analysis filters:

Design example: amplitude responses of the four analysis filters

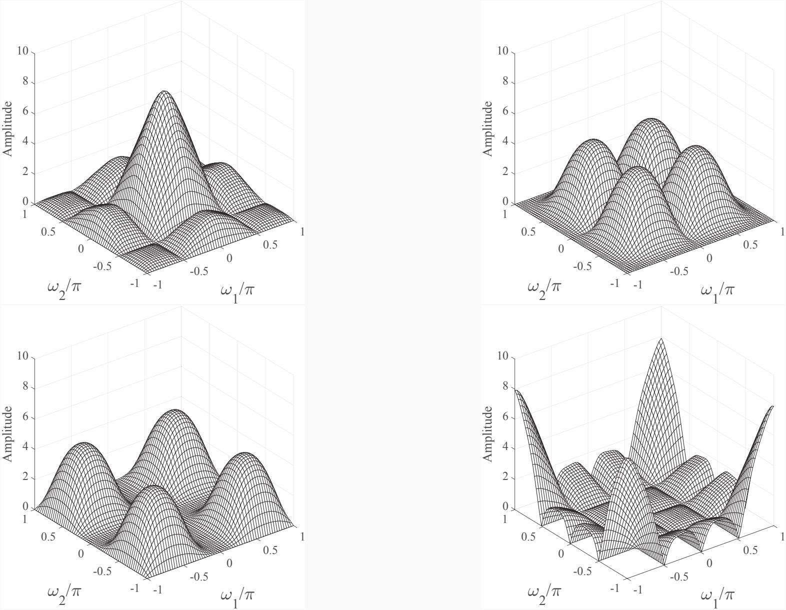

Conclusions and future work

Conclusions

- The 2-D technique of non-separable factorization for 4-th and 8-th chanel PMI LP Q-PUFBs is presented.
- 2-D non-separable FBs perform more efficiently for image coding than separable FBs, because non-separable FBs may have better frequency characteristics
- The factorization structures of 2-D NSQ-PUFB can be easily mapped on the parallel-pipeline processor architecture.

Future work

- Develop FPSoC architecture of image processing system based on the 2-D NSQ-PUFB
- Research image border extension for shown approach

Thank you for attention

Questions?